

# 地盤の不整形性が地盤の非線形応答に与える影響

NONLINEAR SITE RESPONSE AFFECTED BY IRREGULAR TOPOGRAPHY

茂木秀則 (理工学研究科・講師)

Hidenori Mogi, Lecturer, Graduate School of Science and Engineering

## 1 Introduction

It is well known that ground with irregular topographic surfaces causes complicated seismic responses. The process of generating such complex responses, however, is not yet clear. In this study, we investigated the excitation process of complicated seismic responses induced by irregular ground surfaces in terms of the contribution of scattered waves by using the direct boundary element method and Neumann series expansion.

## 2 Boundary Element Method

Displacements of SH-waves with harmonic time-dependence of angular frequency  $\omega$ ,  $\exp(i\omega t)$ , satisfy the Helmholtz equation

$$\{\nabla^2 + k_\beta^2\} u(\mathbf{X}) = 0, \quad (1)$$

where  $u(\mathbf{X})$  is the displacement at arbitrary point  $\mathbf{X} = (x, z)$ ,  $k_\beta = \omega/\beta$  is the wavenumber of the S-wave, and  $\beta$  is the S-wave velocity.

From Eq. (1), the following integral equation can be obtained:

$$\frac{1}{2} u(\mathbf{Y}) + \text{v.p.} \int_\Gamma q^*(\mathbf{X}, \mathbf{Y}) u(\mathbf{X}) d\Gamma(\mathbf{X}) = v(\mathbf{Y}) \quad (2)$$

where  $\mathbf{X}$  and  $\mathbf{Y}$  are points on boundary  $\Gamma$ , v.p. is the Cauchy principal-value integral,  $v(\mathbf{Y})$  is the displacement of the incident wave, and  $q^*(\mathbf{X}, \mathbf{Y})$  is the fundamental solution.

By the discretization of Eq. (2), we get the following simultaneous equations:

$$\mathbf{v} = \frac{1}{2} \mathbf{H}' \mathbf{u} \quad (3)$$

where  $\mathbf{H}'$  is the boundary element matrix whose ele-

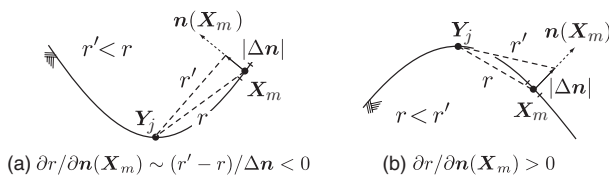


Figure 1: Sign of inclination factor  $\partial r / \partial n$  for ground that is (a) concave and (b) convex.

ments are given by

$$h'_{jm} = 2 \int_{\Gamma_m} \frac{ik_\beta}{4} H_1^{(2)}(k_\beta r) \frac{\partial r}{\partial n(\mathbf{X})} d\Gamma(\mathbf{X}) + \delta_{jm}. \quad (4)$$

## 3 Formulation of Scattered Waves

Applying the Neumann series expansion to Eq. (3), the unknown displacement  $\mathbf{u}$  can be expressed in the form

$$\mathbf{u} = (\mathbf{E} - \mathbf{H})^{-1} 2\mathbf{v} = 2\mathbf{E}\mathbf{v} + 2\mathbf{H}\mathbf{v} + \dots \quad (5)$$

where  $\mathbf{E}$  is a unit matrix, and  $\mathbf{H}$  satisfies

$$\mathbf{H}' = \mathbf{E} - \mathbf{H}. \quad (6)$$

The non-diagonal elements of  $\mathbf{H}$  are given by

$$h_{jm} = -2 \int_{\Gamma_m} \frac{ik_\beta}{4} H_1^{(2)}(k_\beta r) \frac{\partial r}{\partial n(\mathbf{X})} d\Gamma(\mathbf{X}), \quad (7)$$

while the diagonal components are zero.

The first term of the series,  $2\mathbf{E}\mathbf{v}$ , represents the response at the ground surface induced only by an incident wave (i.e., without scattered waves). The second term,  $2\mathbf{H}\mathbf{v}$ , can be understood as first-order scattered wave, because this term represents the responses to the cylindrical waves coming from the other parts of the ground surface.

Eq. (3) can also be modified as

$$\mathbf{u} = \mathbf{H}'^{-1} 2\mathbf{v} = \mathbf{E} 2\mathbf{v} + \mathbf{S} 2\mathbf{v} \quad (8)$$

where

$$\mathbf{S} = \mathbf{H}'^{-1} - \mathbf{E}. \quad (9)$$

The second term,  $\mathbf{S} 2\mathbf{v}$ , represents total scattered wave including multiple scattering generated at the irregular ground surface.

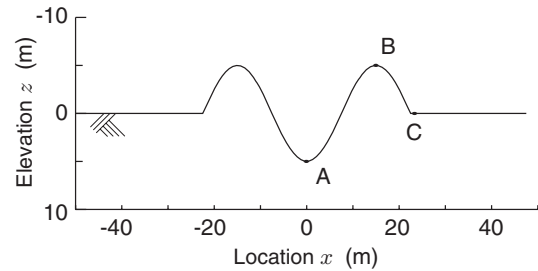


Figure 2: The sinusoidal ground model used in this study with the location of reference points A, B, and C.

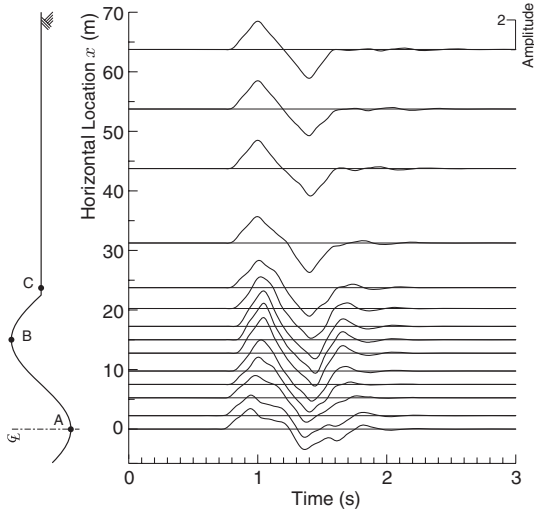


Figure 3: Waveforms induced by a vertical incident wave with double-triangular time function.

## 4 Inclination Factor and Polarity of Scattered Waves

The mathematical expression of the first-order scattered wave given by Eq. (7) has two factors: the former  $-iH_1^{(2)}(k_\beta r)$  represents a cylindrical wave propagating from the source node where the incident wave impinges, and the latter,  $\partial r/\partial n(\mathbf{X})$ , represents amplitude of the secondary wavelet propagating in each direction. We refer to the latter as the inclination factor.

For example, for reference point  $\mathbf{Y}_j$  and source point  $\mathbf{X}_m$  located on concave topography as shown in Figure 1a, the waveform of the first-order scattered wave at reference point  $\mathbf{Y}_j$  has negative polarity (opposite polarity to that of incident wave  $v_m$ ) because the integrand of Eq. (7) for  $r \ll 1$  becomes

$$-\frac{ik_\beta}{2} H_1^{(2)}(k_\beta r) \frac{\partial r}{\partial n(X)} \sim -\frac{k_\beta}{2} Y_1(0) \frac{\partial r}{\partial n(X)} = -\infty \quad (10)$$

for the negative inclination factor  $\partial r/\partial n(\mathbf{X})$ . On the contrary, for the points on convex topography (Fig. 1b), the polarity of the first-order scattered wave is positive (same polarity as that of the incident wave) because of their positive inclination factor.

## 5 Ground Model

A ground model with a sinusoidal surface having three reference points A, B, and C is shown in Figure 2 in order to examine the characteristic responses of the ground surface. The model was assumed to be an isotropic homogeneous elastic half-space with S-wave velocity of 100 m/s. The length and amplitude of the sinusoidal part are 45 m and 5 m, respectively.

## 6 Surface Response

Figure 3 shows waveforms at various positions obtained using the conventional BEM.

In this figure, we can see that the response at the trough (point A) has smaller amplitude but a more complicated shape with several bends compared to those at the other locations. These bends can be inferred as the arrivals of scattered waves and will be discussed in detail in the next section.

Meanwhile, the waveform at the peak (point B) shows larger amplitude: this result is consistent with previous observations indicating that amplification occurred at the top of a hill or mountain.

## 7 Scattered waves arriving at a trough

Figure 4 plots waveforms of the scattered waves emanating from each part of the ground surface (source node) and observed at point A. The waveforms are plotted on the horizontal position of the source node.

In Figure 4(a), we can observe that (1) the bend after the peak can be attributed to the scattered waves coming from the slope of the convex part facing point A (indicated by 1 on the ground model shown to the left side of the vertical axis). (2) The decrease in the peak amplitude is caused by the scattered waves coming from the ground surface close to point A (indicated by 2 on the ground model).

In Figure 4(b), the first-order scattered waves coming from the slope of the convex part (1) have positive polarity and time delays. Considering Eq. (7), it is well understood that the positive polarity is due to the positive inclination factor at the source node for point A, and the delays are primarily caused by the wave propagation from the source nodes to point A. The scattered waves from the nearby surface (2) can also be attributed to short distance  $r$  and the negative inclination factor  $\partial r/\partial n(\mathbf{X})$ .

## 8 Scattered waves arriving at a peak

Point B is located at the peak of the sinusoidal ground model and represents mountains or areas with higher elevations.

In Figure 5, we can see that the waveforms of the total and first-order scattered waves from this part (indicated by 1) have positive polarity, and their peak amplitudes appear almost at the same time as that of the incident wave. The large peak amplitudes and the timing of the arrivals of these scattered waves can be attributed to short distance  $r$  for the same reason discussed in the previous section for point A; the positive polarity is due to the positive inclination factor around point B. (see Fig. 1b). Thus, these scattered waves always have positive polarity, so they always enhance the amplitude of

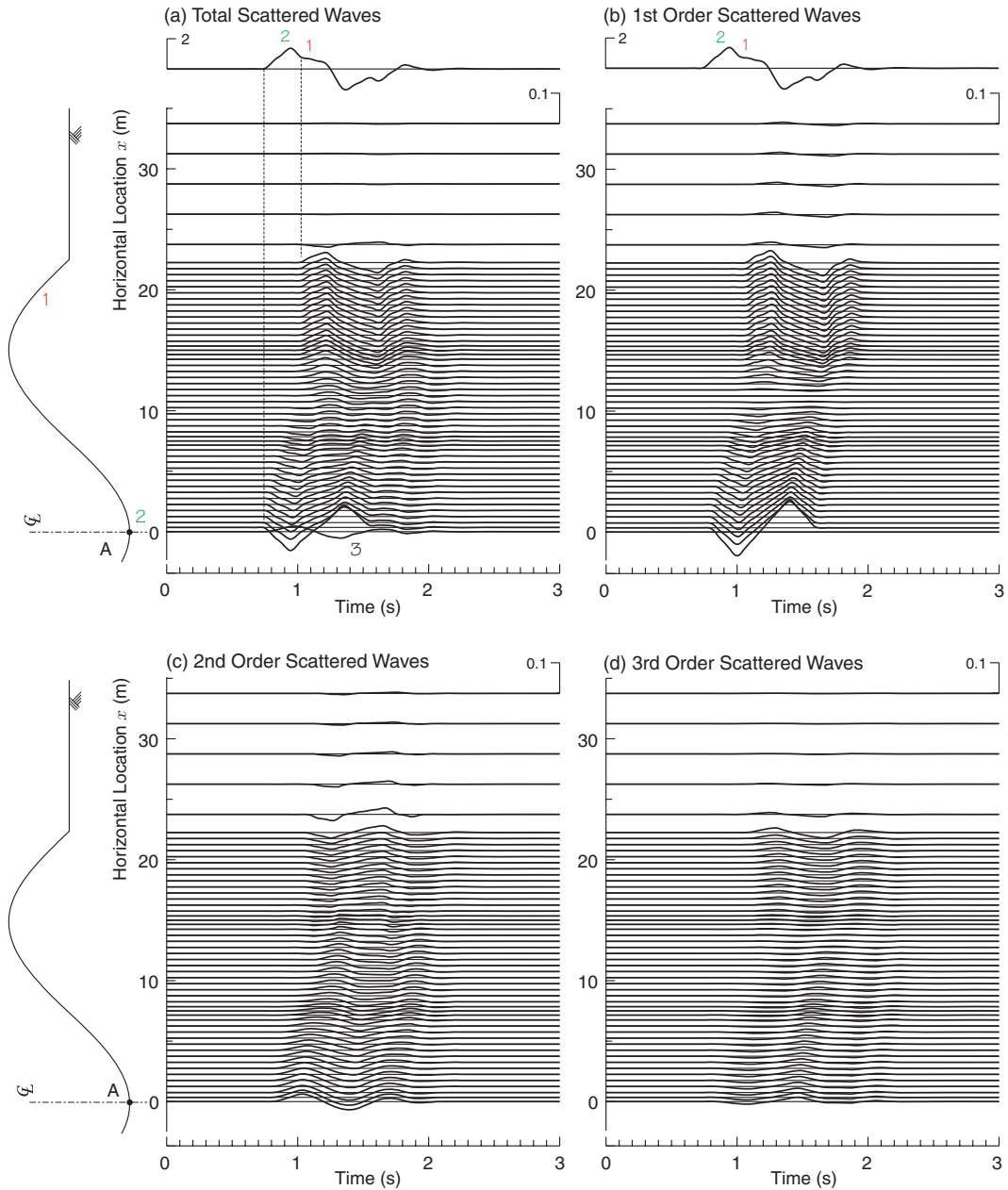


Figure 4: Waveforms of the scattered waves emanating from each part of the ground surface (source node) and arriving at point A. Waveforms are plotted on the horizontal position of the source node where the scattered wave emanates from. In these figures, (a) shows the total scattered waves, and (b) to (d) show the first- to third-order scattered waves, respectively. The response at point A shown in Fig. 3 is also plotted at the top of the figure.

the response at the peak due to constructive interference no matter what impinging occurs from incident waves. This is an explanation for amplified seismic responses observed at a peak from the viewpoint of the contribution of scattered waves.

In Figure 5a, we can also observe the total scattered waves from the flank of the convex part on the left (indicated by 2) as well as the flat areas (indicated by 3); the former implies the propagation of the scattered waves beneath the trough (indicated by 4). This observation highlights that diffraction has to be considered in discussions on seismic response at ground surfaces with irregular topography.

## 9 Conclusion

We analyzed scattered waves induced by ground surface irregularities and examined the excitation process of the complicated seismic response of the ground. The major conclusions of this study are enumerated as follows:

- 1) The contribution of the scattered waves was formulated based on the BEM and Neumann series expansion. By using this method, the surface response of the ground can be decomposed into an incident wave and scattered waves in the order that represents the number of reflections at the ground surface,

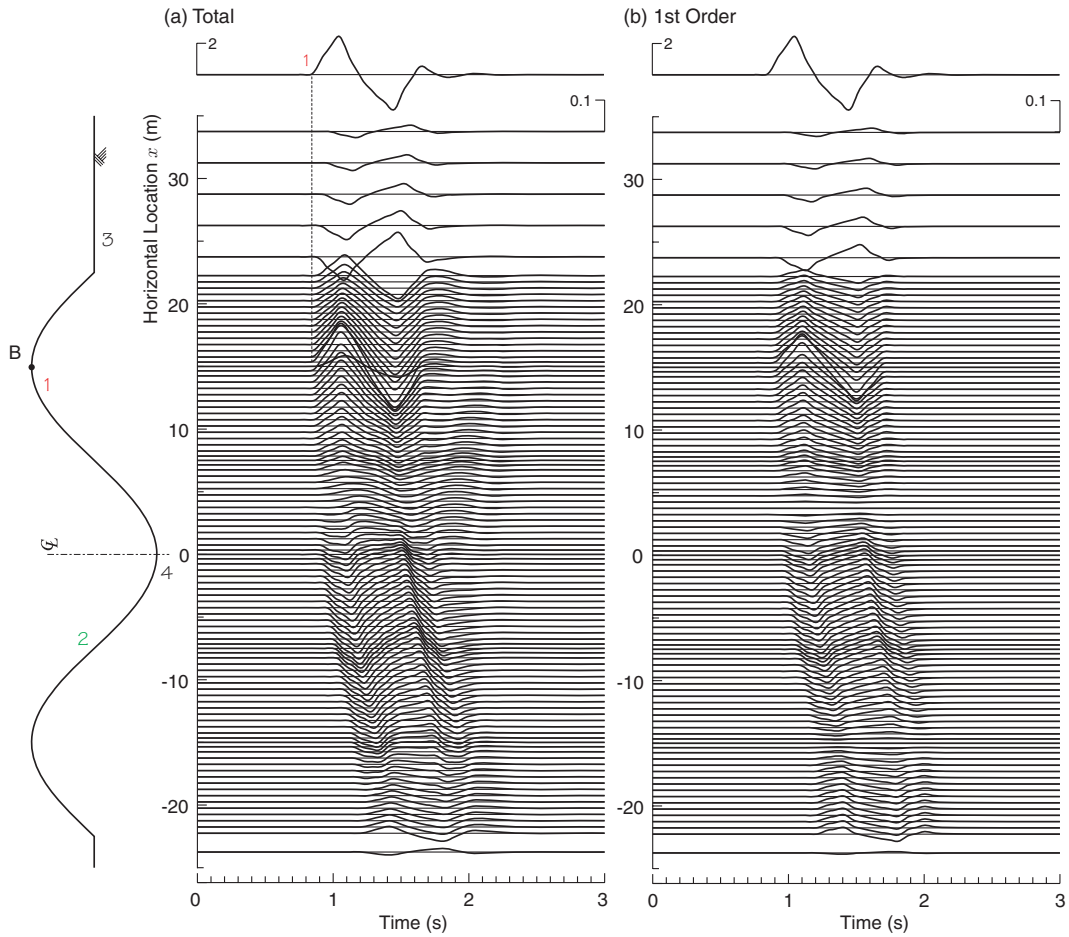


Figure 5: Waveforms of (a) total and (b) first-order scattered waves arriving at point B. The total response waveform at point B is also shown at the top of the figure in the same manner as in Fig. 4.

- 2) The mathematical expression of the first-order scattered waves consists of the inclination factor and the wave function of secondary wavelets, which is similar to that of the Huygens-Fresnel principle,
- 3) The inclination factor is simply given by the term  $\partial r / \partial n$ , and it is an effective index to evaluate the amplitude of scattered waves.
- 4) At the trough (point A), the contribution of the first-order scattered waves consists mainly of the contribution from (1) the slope of the convex part facing the reference point and (2) around the reference point on the concave part. The former scattered waves (1) have positive polarity because of the positive inclination factor and appear much later than the arrival of the incident wave due to wave propagation from the source points. In contrast, the latter (2) have negative polarity because of the negative inclination factor, and appear almost at the same time as the arrival
- 5) At the peak of the mountain (point B), large-amplitude first-order waves scattered from a nearby surface are observed. These scattered waves have positive polarity and appear almost at the same time as the arrival of the incident wave because of the positive inclination factor and the short propagation distance. Therefore, these scattered waves always cause constructive interference with the incident wave at a peak.
- 6) At the peak of the mountain (point B), large-amplitude first-order waves scattered from a nearby surface are observed. These scattered waves have positive polarity and appear almost at the same time as the arrival of the incident wave because of the positive inclination factor and the short propagation distance. Therefore, these scattered waves always cause constructive interference with the incident wave at a peak.
- 7) Thus, the Neumann series expansion of the BEM matrix can reveal the excitation process of the complicated response observed in an irregular topography by decomposing the response into an incident wave and scattered waves.

In the numerical analysis using a sinusoidal ground model, we pointed out the following:

- 4) The first-order scattered waves dominate the other higher-order ones; therefore, we can investigate the characteristics of the total scattered waves based only on the property of the first-order scattered waves,
- 5) At the trough (point A), the contribution of the first-order scattered waves consists mainly of the contribution from (1) the slope of the convex part facing the reference point and (2) around the reference point on the concave part. The former scattered waves (1) have positive polarity because of the positive inclination factor and appear much later than the arrival of the incident wave due to wave propagation from the source points. In contrast, the latter (2) have negative polarity because of the negative inclination factor, and appear almost at the same time as the arrival

of the incident wave because of the short propagation distance. Therefore, these scattered waves always cause destructive interference with the incident wave at a trough; and

- 6) At the peak of the mountain (point B), large-amplitude first-order waves scattered from a nearby surface are observed. These scattered waves have positive polarity and appear almost at the same time as the arrival of the incident wave because of the positive inclination factor and the short propagation distance. Therefore, these scattered waves always cause constructive interference with the incident wave at a peak.
- 7) Thus, the Neumann series expansion of the BEM matrix can reveal the excitation process of the complicated response observed in an irregular topography by decomposing the response into an incident wave and scattered waves.

**References** 1) Boore, D. M. (1972), A note on the effect of simple topography on seismic SH waves, *Bull. Seism. Soc. Am.*, **62**, 1, 275–284. 2) Aki, K. (1989), Local site effects on ground motion, *Earthquake Engineering and Soil Dynamics 2, Recent advances in ground-motion evaluation*, ASCE, 103–155. 3) Brebbia, C. A. and S. Walker (1980), *Boundary element techniques in engineering*, Butterworth & Co. Ltd. 4) Kato, T. (1980), *Perturbation theory for linear operators*, 2nd Ed., Springer-Verlag.